Pragya Darshan 2023, 5(1): 58-63
ISSN: 2542-2634 (print)

Research Article

Numerical Approach of Single-Junction InGaN Solar Cell Affected by Carrier Lifetime and Temperature

[1, 2]D. Parajuli*, 1Viplav Bhandari, [3]Devendra K. C., [1]Ajita Thapaliya, [1]Amrit Subedi, [1]Amrit Dhakal, [1]Sandip Dangi, [1]Rabina Koirala, [1]Manish Bhatta

[1]Department of Physics, Tri-Chandra Multiple Campus, Ghantaghar, Kathmandu
[2]Research Center for Applied Science and Technology, Tribhuvan University, Kirtipur, Nepal.
[3]Myrveien 13, 9740 Lebesby, Norway
**Corresponding author email:* deepenparaj@gmail.com

Abstract

The PC1D simulation aand origin software were successfully used for the study of Carrier Lifetime and Temperature effect on InGaN Single-Junction Solar Cell. For the simulation, the total device area was 100 cm^2, dielectric constant 13.1, band gap 1.35eV, intrinsic constant is 1×10^{10} cm^{-3}, doping concentration is $1\times10^{17}cm^{-3}$, electron number and hole number 1000 and 170 respectively, and the refractive index was 3.58. The optimized temperature and bulk recombination were 25°C and 1000μs respectively along with the efficiency of 18.258 % for both n and p – InGaN solar cell. Several graphs were plotted under the following conditions: a) bulk recombination time of p-InGaN and temperature are kept constant at 1000 μs and 25°C, the variation of bulk recombination time of n – type InGaN solar cell with base current and voltage, maximum current and voltage, and efficiency and maximum power were studied. b) bulk recombination time of n-InGaN and temperature are kept constant at 1000 μs and 25°C, the variation of bulk recombination time of p – type InGaN solar cell with base current and voltage, maximum current and voltage, and efficiency and maximum power were studied.

Keywords: *InGaN solar cell, single junction, bulk recombination, PC1D.*

Introduction

With the development of technologies, new materials has been developed especially in energy efficient devices. There are two aspects of energy management. Either using efficient devices or generation of energy sources both of which were adopted by us. For the development of energy efficient devices, we have conducted investigations on different materials like, Ferrites [1, 2, 3–10, 11–15,], MXenes(D. Parajuli, 2018; D. Parajuli et al., 2023; D. Parajuli, Murali, K. C, et al., 2022; D Parajuli et al., 2019; Deependra Parajuli & Samatha, 2022), electrodes (D. Parajuli, Murali, Samatha, et al., 2022; D. Parajuli, Taddesse, Murali, Veeraiah, et al., 2022) etc. For the energy sources investigation we have gone through different alternative energy approaches mainly in solar cells [21–23] etc. As our global energy expenditure increases exponentially, it is apparent that renewable energy solution must be utilized. Solar PV technology is the best way to utilize the unlimited solar energy. The InGaN is a recently developed novel solar cell material for its promising tunable band gap of 0.7 eV to 3.4 eV for the realization of high efficiency tandem solar cells in space and terrestrial applications(Akter, 2014). The III-nitride semiconductor material system, which consists of InN, GaN, AlN and their alloys, offers a substantial potential in developing ultra-high efficiency photovoltaics mainly due to its wide range of direct-band gap, and other electronic, optical and mechanical properties. However, this novel InGaN material system possesses challenges from theoretical, as well as technological standpoints, which are further extended into the performance of InGaN devices. The InxGa (1-x)N material system is a promising candidate for developing high-efficiency PV systems. Research involving InxGa (1-x) N photovoltaic devices is still in its initial stages. Since the first proposal in 2003 to use InxGa (1-x)N for solar cell applications, substantial efforts have already been made in this research space (Honsberg et al., 2004). The first device showing PV response was reported in 2007 [26]. Although InGaN solar cells are still not fully developed, various theoretical models and numerical simulations have been conducted to investigate the performance of single- and multiple-junction InGaN solar cells (Feng et al., 2010; Hsu & Walukiewicz, 2008; Shen et al., 2008; Zhang et al., 2007). In 2011, S. Ben Machiche has achieved efficiency of 24.88% for single junction InGaN solar cell and efficiency of 34.34% and 37.15% for double junction and triple junction tandem solar cell respectively (Bouzid & machiche, 2011).

There is greater loss in efficiency due to the recombination of charge carriers. The solar radiations reception also depends in many parameters including geographical values. The reflectance, thermodynamic efficiency, charge carrier separation efficiency charge carrier collection efficiency, conduction efficiency are key factors affecting the efficiency of a solar cell system(Green, 1981). The recombination losses are due to quantum efficiency, V_{OC} ratio, and fill factor values. Resistive losses are predominantly accounted for by the fill factor value (Kumar, 2017), but also contribute to the quantum efficiency and V_{OC} ratio values. The highest known efficiency of solar cell was 47.1% was achieved by the use of multi-junction concentrator solar cells, developed at National Renewable Energy Laboratory, Golden, Colorado, USA (Geisz et al., 2018; *Photovoltaic Cell Conversion Efficiency Basics*, 2014).

There are many simulation tools for the study of device simulations like Silvaco TCAD, SCAP-1D, GVPDM, AFORS-HIT, PC1D etc. In this work, PCID simulation is used for the study of InGaN single junction solar cell. The aim of this simulation work is to obtain the maximum conversion efficiency of InGaN single-junction solar cell with the best structure parameters. The effects of the carrier lifetime of each layer on the electrical parameters of the solar cell, such as the short circuit current (Isc),

the open circuit voltage (V), the fill factor (FF), and the conversion efficiency (n), were investigated. Furthermore, the effects of temperature on the conversion efficiency of the single-junction InGaN solar cell were also studied.

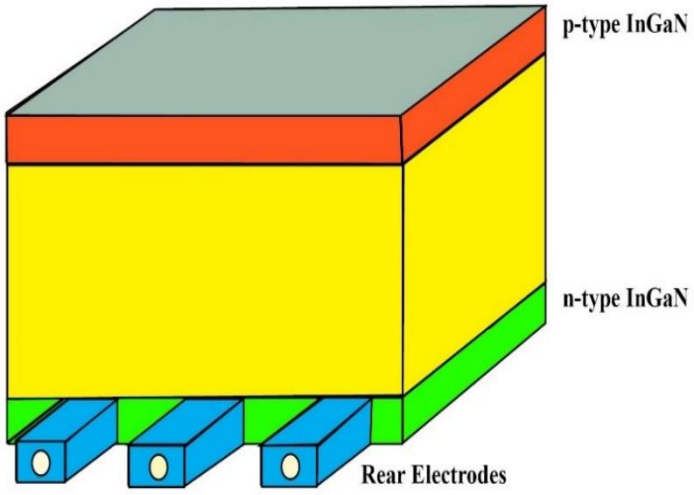

Fig. 1: A 3D schematic diagram of proposed p–n InGaN homojunction solar cell

Methods of Analysis

The PC1D simulation software is used for the computation of the solar cell parameters due to it's free of cost, speed, user interface and updated cell model. PC1D is a three step process: 1. Setting up the simulation parameters which includes the device and material parameters, and the excitation to be applied to the device. 2. Running the simulation. 3. Examining the results. In addition, we have used ORIGIN for plotting graph. We have used the free version of this software. There is also the data analysis facility in origin. In the analysis, the statistics, signal processing and curve fitting option. It can imports, ASCII text, Excel, NITDM etc. and can export the images in JPEG, GIF, EPS, TIFF…etc. In this study, we have considered the effect of temperature, bulk combination in the efficiency of the InGaN solar cell. For device area, 100 cm^2, different sets of reading can be taken and plotted graph between base current and base voltage for different temperatures. Similar set of graphs under the similar input parameters can be drawn for various bulk recombination (carrier lifetime).

The efficiency of a solar cell is determined as the fraction of incident power which is converted to electricity and is defined as:

$$P_{max} = V_{oc} I_{sc} FF$$

$$\eta = V_{oc} I_{sc} FF / P_{in}$$

Where: $FF = \frac{P_{MP}}{V_{OC} \times I_{SC}} = \frac{V_{MP} \times I_{MP}}{V_{OC} \times I_{SC}}$, V_{oc} is the open-circuit voltage; I_{sc} is the short-circuit current; FF is the fill factor and η is the efficiency.

The process of taking the highest efficiency for the study of other solar cell parameters is called optimization. In our case, the maximum efficiency was obtained at 25°C with bulk recombination in 1000 µs of P-InGaN and N-InGaN on single junction solar cell which is 18.358.

Result and Discussions

A schematic diagram (3D and 2D) of proposed p–n InGaN homojunction solar cell are shown in figure 1 and 2 respectively with P-layer and n-layer having thickness of 120 nm and 270 nm. At the time of simulation, the thicknesses are 0.5 µm and 5 µm respectively.

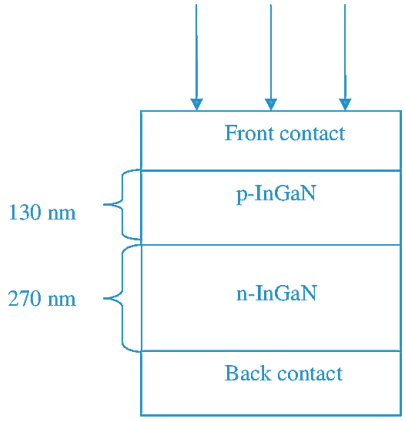

Fig.2: InGaN single junction solar cell

The parameters of the material that are used as the input values in PC1D simulation on InGaN solar cell are listed in table 1.

Table I. Material parameters

Parameter	Value N- InGaN	Value P InGaN
Thickness	0.5 µm	5 µm
Dielectric constant	13.1	13.1
Band gap	1.35eV	1.35eV
Intrinsic conc.	1×10^{10} cm^{-3}	1×10^{10} cm^{-3}
Refractive index	3.58	3.58
Doping	$1\times10^{17}cm^{-3}$	$1\times10^{17}cm^{-3}$
Electron number	1000	1000
Hole number	170	170

Carrier concentration effect of n-InGaN Solar cell

We have taken the thickness and bandgap of the n region as 0.5 µm and 1.35eV respectively to find the optimized value. From our calculation, the maximum efficiency is obtained at 25 °C temperature and the bulk recombination of n - InGaN is 1000µs as optimized value. Different sets are taken for the value of n- InGaN to be 0.001, 0.01, 0.1, 1, 10, 100, 1000 µs respectively. Keeping temperature fixed at 25 °C, we have recorded the changes of current with voltage. All the obtained values are plotted in a graph as shown in figure 3. The base current or the short circuit current (Isc) seems independent with bulk recombination time, while the open circuit voltage is initially constant, drop suddenly to minimum at the bulk combination 10 and then again increases in the same way.

A graph of I_{max} against V_{max} is as shown in figure 4. The P_{max} and its efficiency initially increases and becomes constant with the bulk recombination. The variation of bulk recombination time of n - InGaN was done at the constant value of temperature and p - InGaN bulk recombination.

Similarly, the graph of maximum power and efficiency with bulk recombination for n-InGaN solar cell is as shown in figure 5. In the figure, the power is increasing more rapidly with bulk recombination than the efficiency and finally both attains steady state. The bulk recombination at 10 (μs) show significance change in all the graphs.

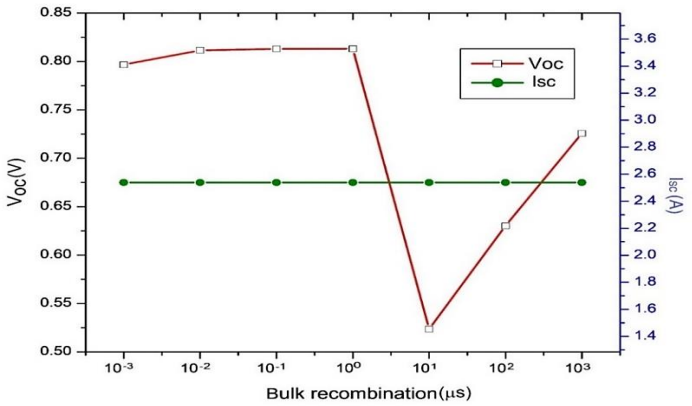

Fig. 3: Graph of variation short circuit and open circuit voltage with bulk recombination of n –InGaN

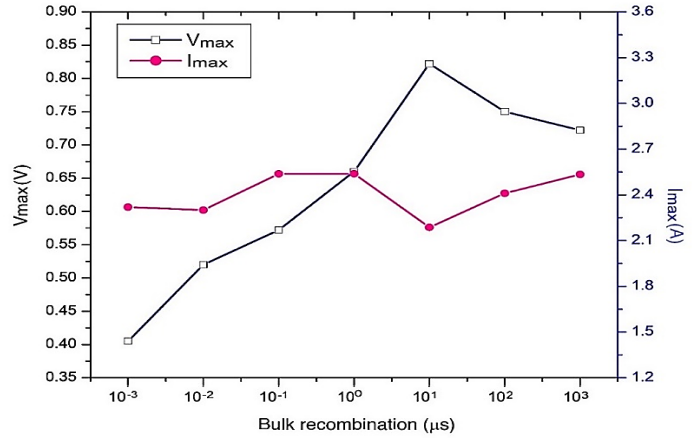

Fig.4: Graph between I_{max} and V_{max} with bulk recombination of n-InGaN

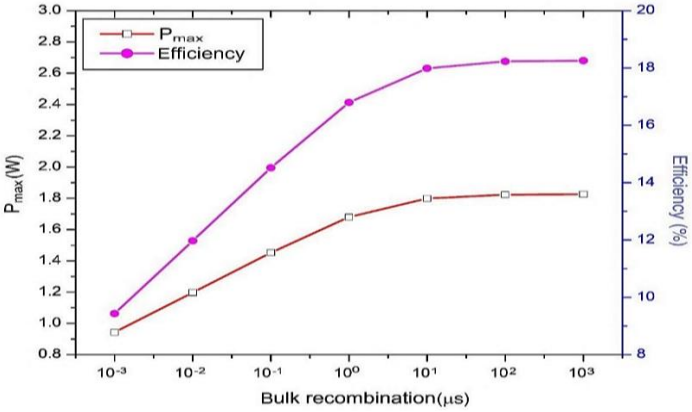

Fig. 5: Graph between Pmax and efficiency with bulk recombination of n-InGaN

Carrier concentration effect on p -InGaN Solar cell

The input values for the optimization of p-InGaN solar cell were 0.5 μm and 1.35eV for thickness and bandgap of the p region respectively. For the optimization, it is assumed that proposed cell has maximum efficiency in the active region. As in the n-type carriers, the bulk recombination time for p-InGaN was varied from 0.001, 0.01, 0.1, 1, 10, 100, 1000 μs respectively.

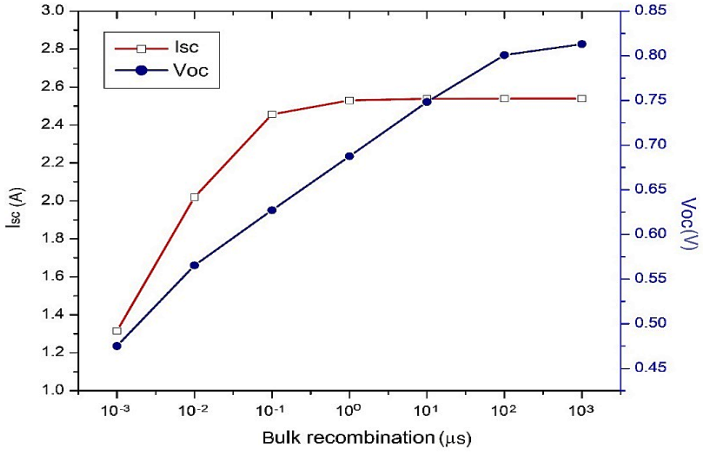

Fig. 6: Graph between the base voltage and current with bulk recombination variation

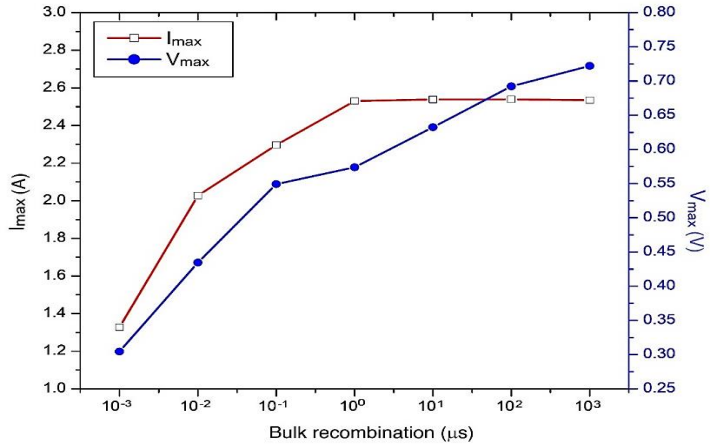

Fig. 7: Graph between I_{max} and V_{max} with bulk recombination of n-InGaN

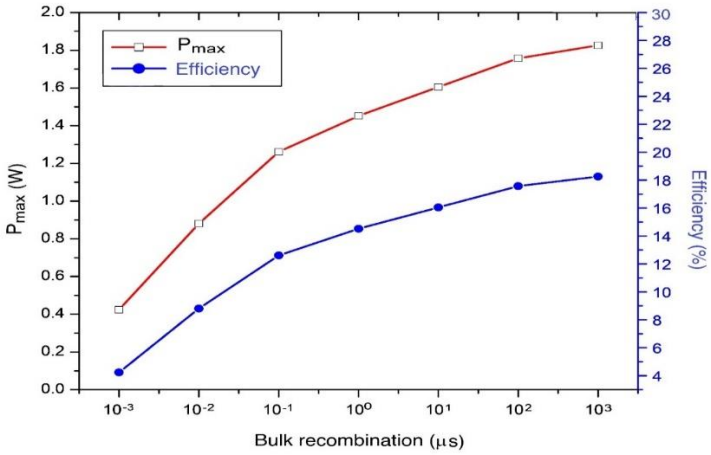

Fig. 8: Graph between P_{max} and efficiency with bulk recombination in p-region

Similarly, the graph of bulk recombination time with maximum current and voltage at constant temperature and n-type bulk recombination is as shown in figure 7. The maximum current and maximum voltage show the same trend with bulk recombination as for Isc and Voc against bulk recombination.

In the same way, the graph between maximum power and efficiency with bulk recombination of p-type under the same condition is shown in figure 8. The power is increasing more rapidly than efficiency with bulk combination.

Impact of temperature

In this case, we have studied the change in various solar cell parameters with the variation in temperature. Here, both the n and p-type bulk recombination time are kept constant at 1000 µs. We have taken different values of short circuit current and open circuit voltage at various temperature ranging from 25 °C to 50°C. The obtained values were plotted in a graph as shown in figure 9. The open circuit voltage is decreasing and the short circuit current is increasing with the temperature. The increasing current with temperature show the semiconducting nature of the system.

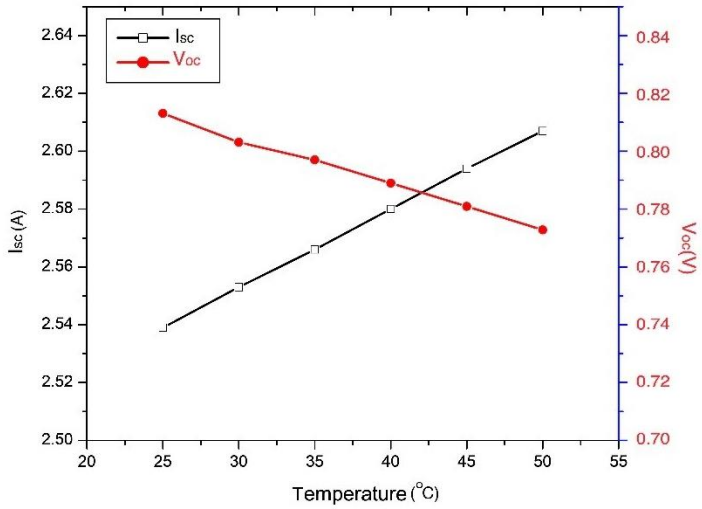

Fig. 9: Graph between I_{sc} and V_{oc} with temperature

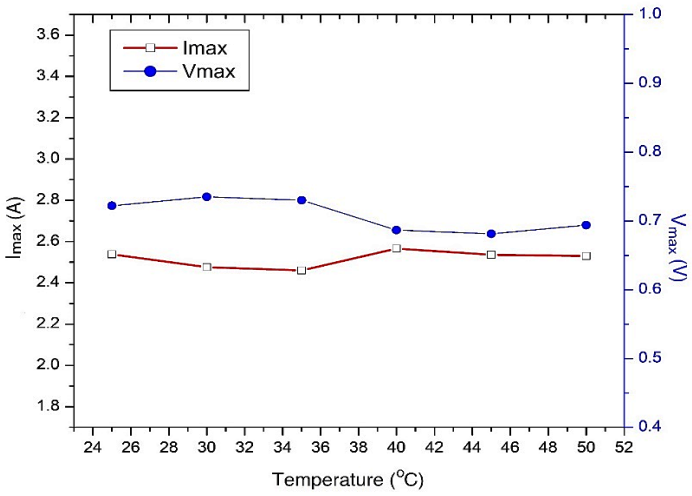

Fig. 10: Graph between Imax and Vmax with temperature

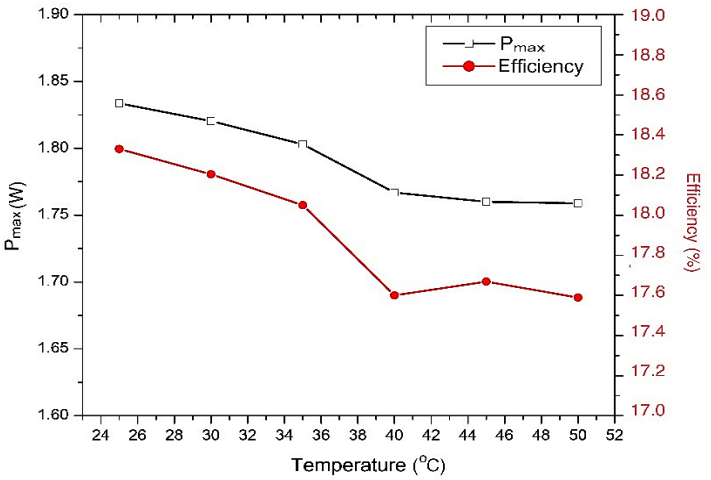

Fig.11: Graph between Pmax and efficiency with temperature

Similarly, the variation of temperature with maximum voltage and current for p-type InGaN is as shown in figure 10. The current is increasing and voltage is decreasing with the temperature and finally both attain the steady values. The variation of temperature with maximum power and the efficiency is as shown in figure 11. Both the efficiency and maximum power are decreasing with the temperature indicating that the solar cell in not good at higher temperature.

Optimization

In this section, two steps are performed,

1) bulk recombination time of p-InGaN and temperature are kept constant at 1000 µs and 25°C, the variation of bulk recombination time of n – type InGaN solar cell with base current and voltage, maximum current and voltage, and efficiency and maximum power were studied.
2) bulk recombination time of n-InGaN and temperature are kept constant at 1000 µs and 25°C, the variation of bulk recombination time of p – type InGaN solar cell with base current and voltage, maximum current and voltage, and efficiency and maximum power were studied.

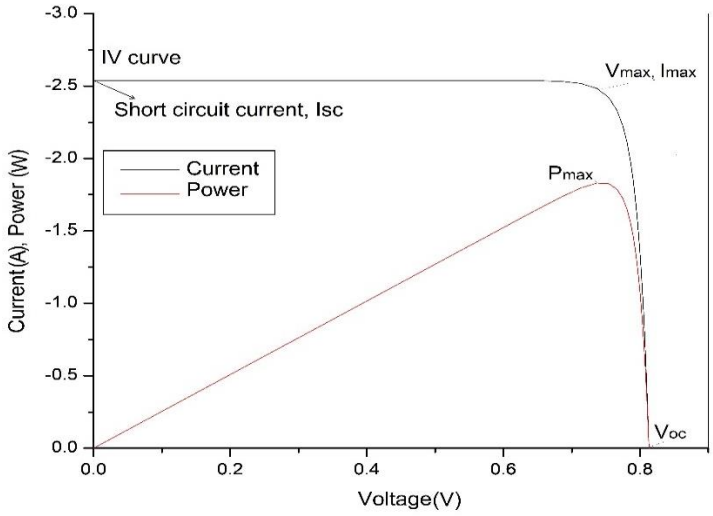

Fig. 12: Base I-V/Power curve

For the InGaN simulation, the n - InGaN layer thickness was 0.5 μm, the p - InGaN layer thickness was 5 μm, the doping concentrations for these layers are 1×10^{17} cm^{-3}, dielectric constant is 13.1, bad gap 1.35eV, intrinsic constant 1×10^{10} cm^{-3}, refractive index 3.58, electron number and hole number 1000 and 170. The obtained results were extracted from the *I-V* curve characteristics for the model as shown in figure 12. The open-circuit voltage (V_{oc}), short-circuit current (I_{sc}), and the efficiency of this initial simulation were found to be 0.8131V, 2.539A, and 18.26 % respectively. The maximum power is obtained from the figure. After all, the optimized value of temperature and bulk recombination were found to be 25°C and 1000 µs respectively.

Conclusions

The PC1D simulation and origin software were successfully used for the study of Carrier Lifetime and Temperature effect on InGaN Single-Junction Solar Cell. For the simulation, the total device area was 100 cm^2, dielectric constant 13.1, band gap 1.35eV, intrinsic constant is 1×10^{10} cm^{-3}, doping concentration is $1\times10^{17}c$m^{-3}, electron number and hole number 1000 and 170 respectively, and the refractive index was 3.58. The optimized temperature and bulk recombination were 25°C and 1000µs respectively along with the efficiency of 18.258 % for both n and p – InGaN solar cell. Several graphs were plotted under the following conditions:

1) bulk recombination time of p-InGaN and temperature are kept constant at 1000 µs and 25°C, the variation of bulk recombination time of n – type InGaN solar cell with base current and voltage, maximum current and voltage, and efficiency and maximum power were studied.
2) bulk recombination time of n-InGaN and temperature are kept constant at 1000 µs and 25°C, the variation of bulk recombination time of p – type InGaN solar cell with base current and voltage, maximum current and voltage, and efficiency and maximum power were studied.

References

Akter, N. (2014). Design and Simulation of Indium and Indium Gallium Nitride Multijunction Tandem Solar Cells. *International Journal of Research in Engineering and Technology*, *03*(01), 315–321. https://doi.org/10.15623/IJRET.2014.0301056

Bouzid, F., & machiche, S. Ben. (2011). Potentials of Inx Ga1-x N photovoltaic tandems. *Https://Library.Crti.Dz/*, *14*(1), 47–56. https://library.crti.dz/jr1315

Chandramouli, K., Suryanarayana, B., Babu, T. A., Raghavendra, V., Parajuli, D., Murali, N., Malapati, V., Mammo, T. W., Shanmukhi, P. S. V., & Gudla, U. R. (2021). Synthesis, structural and antibacterial activity of pure, Fe doped, and glucose capped ZnO nanoparticles. *Surfaces and Interfaces*, *26*, 101327. https://doi.org/10.1016/J.SURFIN.2021.101327

Chandramouli, K., Suryanarayana, B., Phanidhar Varma, P. V. S. K., Raghavendra, V., Emmanuel, K. A., Taddesse, P., Murali, N., Wegayehu Mammo, T., & Parajuli, D. (2021). Effect of Cr3+ substitution on dc electrical resistivity and magnetic properties of Cu0.7Co0.3Fe2−xCrxO4 ferrite nanoparticles prepared by sol-gel auto combustion method. *Results in Physics*, *24*, 104117. https://doi.org/10.1016/J.RINP.2021.104117

Devendra, K. C., Shah, D. K., Wagle, R., Shrivastava, A., & Parajuli, D. (2020). Ingap window layer for gallium arsenide (Gaas) based solar cell using pc1d simulation. *Journal of Advanced Research in Dynamical and Control Systems*, *12*(7 Special Issue), 2878–2885. https://doi.org/10.5373/JARDCS/V12SP7/20202430

Feng, S. W., Lai, C. M., Chen, C. H., Sun, W. C., & Tu, L. W. (2010). Theoretical simulations of the effects of the indium content, thickness, and defect density of the i-layer on the performance of p-i-n InGaN single homojunction solar cells. *Journal of Applied Physics*, *108*(9), 093118. https://doi.org/10.1063/1.3484040

Geisz, J. F., Steiner, M. A., Jain, N., Schulte, K. L., France, R. M., McMahon, W. E., Perl, E. E., & Friedman, D. J. (2018). Building a Six-Junction Inverted Metamorphic Concentrator Solar Cell. *IEEE Journal of Photovoltaics*, *8*(2), 626–632. https://doi.org/10.1109/JPHOTOV.2017.2778567

Green, M. A. (1981). Solar cell fill factors: General graph and empirical expressions. *SSEle*, *24*(8), 788–789. https://doi.org/10.1016/0038-1101(81)90062-9

Gudla, U. R., Suryanarayana, B., Raghavendra, V., Emmanuel, K. A., Murali, N., Taddesse, P., Parajuli, D., Chandra Babu Naidu, K., Ramakrishna, Y., & Chandramouli, K. (2020). Optical and luminescence properties of pure, iron-doped, and glucose capped ZnO nanoparticles. *Results in Physics*, *19*, 103508. https://doi.org/10.1016/J.RINP.2020.103508

Gudla, U. R., Suryanarayana, B., Raghavendra, V., Parajuli, D., Murali, N., Dominic, S., Ramakrishna, Y., & Chandramouli, K. (2021). Structural, optical and luminescence properties of pure, Fe-doped and glucose-capped CdO Semiconductor nanoparticles for their Antibacterial activity. *Journal of Materials Science: Materials in Electronics*, *32*(3), 3920–3928. https://doi.org/10.1007/S10854-020-05135-3/FIGURES/9

Himakar, P., Jayadev, K., Parajuli, D., Murali, N., Taddesse, P., Mulushoa, S. Y., Mammo, T. W., Kishore Babu, B., Veeraiah, V., & Samatha, K. (2021). Effect of Cu substitution on the structural, magnetic, and dc electrical resistivity response of Co0.5Mg0.5-xCuxFe2O4 nanoferrites. *Applied Physics A: Materials Science and Processing*, *127*(5), 1–10. https://link.springer.com/article/10.1007/s00339-021-04521-w

Himakar, P., Murali, N., Parajuli, D., Veeraiah, V., Samatha, K., Mammo, T. W., Batoo, K. M., Hadi, M., Raslan, E. H., & Adil, S. F. (2021). Magnetic and DC Electrical Properties of Cu Doped Co–Zn Nanoferrites. *Journal of Electronic Materials*, *50*(6), 3249–3257. https://link.springer.com/article/10.1007/s11664-021-08760-8

Honsberg, C. B., Jani, O., Doolittle, W. A., Ferguson, I., Honsberg, C., Doolittle, A., Trybus, E., Namkoong, G., Nicole, D., & Payne, A. (2004). InGaN-a new solar cell material Solar City Smart Grid Project View project Metal Modulated Epitaxial growth optimization of nitrides View project InGaN-A NEW SOLAR CELL MATERIAL. *In Proceedings of the 19th European Photovoltaic Science and Engineering Conference, Paris, France*, 15–20.

Hsu, L., & Walukiewicz, W. (2008). Modeling of InGaN/Si tandem solar cells. *Journal of Applied Physics*, *104*(2), 024507. https://doi.org/10.1063/1.2952031

Jani, O., Ferguson, I., Honsberg, C., & Kurtz, S. (2007). Design and characterization of GaN/InGaN solar cells. *Applied Physics Letters*, *91*(13), 132117. https://doi.org/10.1063/1.2793180

Kumar, A. (2017). Predicting efficiency of solar cells based on transparent conducting electrodes. *Journal of Applied Physics*, *121*(1), 014502. https://doi.org/10.1063/1.4973117

P. V. S. K. Phanidhar Varma, B. Suryanarayana, Vemuri Raghavendra, D. Parajuli, N. Murali, K. C. (2020). Effect of Cr substitution on magnetic properties of Co-Cu nano ferrites. *Solid State Technology*, *63*(5), 8820–8827. http://solidstatetechnology.us/index.php/JSST/article/view/7828

Parajuli, D. (2018). First Principles Study of Electronic and Magnetic Properties of Nitinol. *The Journal of University Grants Commission University Grants Commission*, *2*(1), 24–39.

Parajuli, D., Murali, N., K. C, D., Karki, B., Samatha, K., Kim, A. A., Park, M., & Pant, B. (2022). Advancements in MXene-Polymer Nanocomposites in Energy Storage and Biomedical Applications. *Polymers 2022, Vol. 14, Page 3433*, *14*(16), 3433. https://doi.org/10.3390/POLYM14163433

Parajuli, D., Murali, N., & Samatha, K. (2022). Correlation between the Magnetic and DC resistivity studies of Cu substituted Ni and Zn in Ni-Zn ferrites. *BIBECHANA*, *19*(1–2), 61–67. https://doi.org/10.3126/BIBECHANA.V19I1-2.46387

Parajuli, D., Murali, N., Samatha, K., & Veeraiah, V. (2022). Thermal, structural, morphological, functional group and first cycle charge/discharge study of Co substituted LiNi1−x-0.02Mg0.02CoxO2 (x = 0.00, 0.02, 0.04, 0.06, and 0.08) cathode material for LIBs. *AIP Advances*, *12*(8), 085010. https://doi.org/10.1063/5.0096297

Parajuli, D., Raghavendra, V., Suryanarayana, B., Rao, P. A., Murali, N., Varma, P. V. S. K. P., Prasad, R. G., Ramakrishna, Y., & Chandramouli, K. (2021). Corrigendum to "Cadmium substitution effect on structural, electrical and magnetic properties of Ni-Zn nano ferrites" [Results Phys. 19 (2020) 2211-379 103487]. *Results in Physics*, *23*, 103947. https://doi.org/10.1016/J.RINP.2021.103947

Parajuli, D., & Samatha, K. (2021). Morphological analysis of Cu substituted Ni\Zn in Ni-Zn ferrites. *BIBECHANA*, *18*(2), 80–86. https://doi.org/10.3126/BIBECHANA.V18I2.34383

Parajuli, D., Shah, D. K., KC, D., Kumar, S., Park, M., & Pant, B. (2022). Influence of Doping Concentration and Thickness of Regions on the Performance of InGaN Single Junction-Based Solar Cells : A Simulation Approach. *Electrochem*, *3*, 407–415.

Parajuli, D., Taddesse, P., Murali, N., Veeraiah, V., & Samatha, K. (2022). Effect of Zn2+ doping on thermal, structural, morphological, functional group, and electrochemical properties of layered LiNi0.8Co0.1Mn0.1O2 cathode material. *AIP Advances*, *12*(12), 125012. https://doi.org/10.1063/5.0122976

Parajuli, D., Uppugalla, S., Murali, N., Ramakrishna, A., Suryanarayana, B., & Samatha, K. (2023). Synthesis and characterization MXene-Ferrite nanocomposites and its application for dying and shielding. *Inorganic Chemistry Communications*, *148*, 110319. https://doi.org/10.1016/J.INOCHE.2022.110319

Parajuli, D., Vagolu, V. K., Chandramoli, K., Murali, N., & Samatha, K. (2022). Electrical Properties of Cobalt Substituted NZCF and ZNCF Nanoparticles Prepared by the Soft Synthesis Method. *Journal of Nepal Physical Society*, *8*(3), 45–52. https://doi.org/10.3126/JNPHYSSOC.V8I3.50726

Parajuli, D, Kaphle, G. C., & Samatha, K. (2019). First-Principles Study of Electronic and Magnetic Properties of Anatase and its Role in Anatase-Mxene Nanocomposite. *Journal of Nepal Physical Society*, *5*(1), 42–53. https://doi.org/10.3126/JNPHYSSOC.V5I1.26940

Parajuli, D, Murali, N., & Samatha, K. (2021). Structural, Morphological, and Magnetic Properties of Nickel Substituted Cobalt Zinc Nanoferrites at Different Sintering Temperature. *Journal of Nepal Physical Society*, *7*(2), 24–32. https://doi.org/10.3126/JNPHYSSOC.V7I2.38619

Parajuli, D, Vagolu, V. K., Chandramoli, K., Murali, N., & Samatha, K. (2021). Soft Chemical Synthesis of Nickel-Zinc-Cobalt-Ferrite Nanoparticles and their Structural, Morphological and Magnetic Study at Room Temperature. *Journal of Nepal Physical Society*, *7*(4), 14–18. https://doi.org/10.3126/JNPHYSSOC.V7I4.42926

Parajuli, Deependra, & Samatha, K. (2021). Structural analysis of Cu substituted Ni\Zn in Ni-Zn Ferrite. *BIBECHANA*, *18*(1), 128–133. https://doi.org/10.3126/BIBECHANA.V18I1.29475

Parajuli, Deependra, & Samatha, K. (2022). Topological properties of MXenes. In *MXenes and their Composites*. Elsevier. https://doi.org/10.1016/B978-0-12-823361-0.00015-0

Photovoltaic Cell Conversion Efficiency Basics. (2014, October 6). U.S. Department of Energy.

Sankpal, A. M., Kakatkar, S. V., Chaudhari, N. D., Patil, R. S., Sawant, S. R., & Suryavanshi, S. S. (1998). Initial permeability studies on A13+ and Cr3+ substituted Ni-Zn ferrites. *Journal of Materials Science: Materials in Electronics*, *9*(2), 173–179. https://doi.org/10.1023/A:1008884400574

Shah, D. K., KC, D., Parajuli, D., Akhtar, M. S., Kim, C. Y., & Yang, O.-B. (2022). A computational study of carrier lifetime, doping concentration, and thickness of window layer for GaAs solar cell based on Al2O3 antireflection layer. *Solar Energy*, *234*, 330–337. https://doi.org/10.1016/J.SOLENER.2022.02.006

Shen, X., Lin, S., Li, F., Wei, Y., Zhong, S., Shen, A. X., Wan, H., & Li, J. (2008). Simulation of the InGaN-based tandem solar cells. *Https://Doi.Org/10.1117/12.793997*, *7045*, 84–91. https://doi.org/10.1117/12.793997

Zhang, X., Wang, X., Xiao, H., Yang, C., Ran, J., Wang, C., Hou, Q., & Li, J. (2007). Simulation of In0.65Ga0.35 N single-junction solar cell. *Journal of Physics D: Applied Physics*, *40*(23), 7335. https://doi.org/10.1088/0022-3727/40/23/013